

Interactions of Silicate Ions with Zinc(II) and Aluminum(III) in Alkaline Aqueous Solution

Michel R. Anseau,[†] Jennifer P. Leung,[‡] Nita Sahai,[#] and Thomas W. Swaddle^{*‡}

Department of Organic and Biomedical Chemistry, Faculty of Medicine and Pharmacy, NMR and Molecular Imaging Laboratory, University of Mons-Hainaut, 7000 Mons, Belgium, Department of Chemistry, University of Calgary, Calgary, AB, Canada T2N 1N4, and Department of Geology and Geophysics, University of Wisconsin, Madison, Wisconsin 53706-1692

Received April 16, 2005

We present ²⁹Si, ²⁷Al, and ⁶⁷Zn NMR evidence to show that silicate ions in alkaline solution form complexes with zinc(II) (present as zincate, Zn(OH)₃⁻ or Zn(OH)₄²⁻) and, concomitantly, with aluminate (Al(OH)₄⁻). Zincate reacts with monomeric silicate at pH 14–15 to form [(HO)O₂Si–O–Zn(OH)₃]⁴⁻ and with dimeric silicate to produce [HO–SiO₂–O–SiO₂–O–Zn(OH)₃]⁶⁻. The exchange of Si between these free and Zn-bound sites is immeasurably fast on the ²⁹Si NMR time scale. The cyclic silicate trimer reacts relatively slowly and incompletely with zincate to form [(HO)₃Zn{(SiO₃)₃}]⁷⁻. The concentration of the cyclic trimer becomes further depleted because zincate scavenges the silicate monomer and dimer, with which the cyclic trimer is in equilibrium on the time scale of sample preparation. Identification of these zincate–silicate complexes is supported by quantum chemical theoretical calculations. Aluminate and zincate, when present together, compete roughly equally for a deficiency of silicate to form [(HO)₃ZnOSiO₂OH]⁴⁻ and [(HO)₃AlOSiO₂OH]³⁻ which exchange ²⁹Si at a fast but measurable rate.

Introduction

This study was prompted by recent observations that bioactive ceramics such as pseudowollastonite (psW, a high-temperature form of wollastonite, CaSiO₃) promote collagen, hydroxyapatite, and bone nodule formation when they are implanted in mineralized tissues^{1–3} or immersed in osteoblastic cell cultures.^{4–7} The effect is associated with the release of silicate and calcium ions into the physiological

environment, which becomes permanently alkaline locally; thus, the pH may rise as high as 10.5 near the surface of the psW.⁸ Silicon(IV) in experimental animals is known^{9–12} to affect the metabolism of zinc(II), which is essential for the formation of bone matrix constituents.¹³ It is possible that the beneficial action of dietary Si is due in part to the interaction of aqueous silicon(IV) with zinc(II) in the physiological fluid. In the present study, we have sought evidence from nuclear magnetic resonance (NMR) spectroscopy for specific interactions, such as complex formation between silicate anions and zinc(II) in alkaline aqueous solution, similar to those previously established¹⁴ between silicates and aluminum(III). Both Zn^{II} and Al^{III} are amphoteric and are present in alkaline solution as zincate (Zn(OH)_x^{(x-2)-}) and aluminate (Al(OH)₄⁻) anions, respec-

* To whom correspondence should be addressed. E-mail: swaddle@ucalgary.ca. Phone: (403) 220–5358. Fax: (403) 289–9488.

[†] University of Mons-Hainaut.

[‡] University of Calgary.

[#] University of Wisconsin-Madison.

- (1) De Aza, P. N.; Luklinska, Z. B.; Martinez, A.; Anseau, M. R.; Guitian, F.; De Aza, S. *J. Microsc.* **2000**, *197*, 60.
- (2) De Aza, P. N.; Luklinska, Z. B.; Anseau, M. R.; Guitian, F.; De Aza, S. *J. Microsc.* **2001**, *201* (Part 1), 33.
- (3) Sahai, N.; Anseau, M. *Biomaterials* **2005**, *26*, 5763.
- (4) Sarmiento, C.; Luklinska, Z. B.; Brown, L.; Anseau, M. R.; De Aza, P. N.; Hughes, F.; McKay, I. J. *J. Biomed. Mater. Res.* **2004**, *69A*, 351.
- (5) Sarmiento, C. F. de M. Studies of the Expansion of Osteoblast Precursor Cells in Culture and their Interactions with a Novel Bioactive Ceramic, Pseudowollastonite, Ph.D. Thesis, University of London, London, 2001.
- (6) Dufrene, D.; Delloye, C.; De Aza, P. N.; De Aza, S.; Schneider, Y. J.; Anseau, M. *J. Mater. Sci. Mater. Med.* **2003**, *14*, 33.
- (7) Dufrene, D.; Anseau, M.; McKay, I.; De Aza, P.; Delloye, C. *Eur. Cells Mat.* **2002**, *3* (Suppl. 1), 18.

- (8) De Aza, P. N.; Guitian, F.; Merlos, A.; Lora-Tomayo, E.; De Aza, S. *J. Mater. Sci. Mater. Med.* **1996**, *7*, 399.
- (9) Seaborn, C. D.; Nielsen, F. H. *Biol. Trace Elem. Res.* **2002**, *89*, 251.
- (10) Emerick, R. J.; Kayongo-Male, H. *J. Nutr. Biochem.* **1990**, *1*, 35.
- (11) Evenson, D. P.; Emerick, R. J.; Jost, H.; Kayongo-Male, H.; Stewart, S. R. *J. Anim. Sci.* **1993**, *71*, 955.
- (12) Seaborn, C. D.; Nielsen, F. H. *Biol. Trace Elem. Res.* **2002**, *89*, 239.
- (13) (a) National Research Council Subcommittee on Zinc. *Zinc*; University Park Press: Baltimore, 1979. (b) *Zinc and Copper in Medicine*; Karcioğlu, Z. A., Sarper, R. M., Eds.; Charles C. Thomas: Springfield, IL, 1980.
- (14) Swaddle, T. W. *Coord. Chem. Rev.* **2001**, *219–221*, 665.

tively,¹⁵ by analogy with the reactions of silicates with $\text{Al}(\text{OH})_4^-$,¹⁴ the condensation of $\equiv\text{Zn}-\text{OH}$ with $\text{HO}-\text{Si}\equiv$ groups to form zincate-silicate complexes may be anticipated. Furthermore, because malformation or deterioration of bone (osteomalacia) caused by Al^{III} is known to be counteracted by dietary Si^{IV} ,¹⁶ we have also enquired as to whether silicates can form complexes with Zn^{II} and Al^{III} concurrently.

At pH values typically associated with psW implants and immersed bioactive ceramics, zinc(II) shows significant local solubility as $\text{Zn}(\text{OH})_3^-$ ¹⁵ and silicon(IV) is present as $(\text{HO})_3\text{SiO}^-$ and numerous silicate oligomers.^{17–21} Preliminary ²⁹Si NMR studies²² of the aqueous phase of psW suspensions, however, failed to detect the low concentrations of dissolved silicates (total $[\text{Si}] \leq 2 \text{ mmol L}^{-1}$, spread over many different species), and we were obliged, for reasons given below, to resort to highly alkaline solutions of SiO_2 to obtain informative spectra. Consequently, the primary aims of this study were focused on answering the question of whether zincate-silicate complexes can exist at all in aqueous alkaline solution and, if so, to identify the species involved, rather than to simulate $\text{Si}^{\text{IV}}-\text{Zn}^{\text{II}}$ interactions under physiological conditions.

Reports of the existence of $\equiv\text{Si}-\text{O}-\text{Zn}\equiv$ complexes are sparse because there are very few techniques available for their characterization and also because solid $\text{Zn}(\text{OH})_2$ and zinc silicates tend to precipitate.^{23,24} Precipitation can be avoided by resorting to high pH (14 or more) where Zn is freely soluble as $\text{Zn}(\text{OH})_4^{2-}$ and Si is present mainly as $(\text{HO})_2\text{SiO}_2^{2-}$ (the first and second $\text{p}K_a$ values of $\text{Si}(\text{OH})_4$ are 9.7 and 12.5).^{15,17} Zhao et al.,^{25,26} using $[\text{OH}^-]$ of 1–2 mol L^{-1} , were able to make quantitative potentiometric and polarographic measurements on solutions containing $[\text{Si}] \leq 0.5 \text{ mol L}^{-1}$ and $[\text{Zn}] \leq 0.02 \text{ mol L}^{-1}$ that indicated the existence in solution of various silicate-zincate complexes. Zhao et al.^{25,26} proposed the presence of the species $[(\text{HO})_3\text{ZnOSi}(\text{OH})_2\text{O}]^{3-}$ and $[\text{O}(\text{HO})_2\text{SiOZn}(\text{OH})_2\text{OSiO}(\text{OH})_2\text{O}]^{4-}$ (stability constants at 30 °C and ionic strength 5.0 mol L^{-1} given by Zhao et al.²⁶ as $[[(\text{HO})_3\text{ZnOSi}(\text{OH})_3]^{2-}]/[\text{SiO}(\text{OH})_3^-][\text{Zn}^{2+}][\text{OH}^-]^3 = 1.2 \times 10^{16}$ and $[[\text{Zn}(\text{OH})_2(\text{SiO}_2(\text{OH})_2)_2]^{4-}]/[\text{SiO}_2(\text{OH})_2^{2-}]^2[\text{Zn}^{2+}][\text{OH}^-]^2 = 6.2 \times 10^{16}$) as well as $[(\text{HO})_2\text{Zn}_2(\text{Si}_4\text{O}_8(\text{OH})_4)(\text{OH})_4]^{4-}$ and unspecified others. These stability constants are of limited significance

because the speciation of the silicate and silicate-zincate complexes was not corroborated by structural techniques and because degrees of deprotonation higher than those proposed would be expected at the reported alkali concentrations ($\geq 1 \text{ mol L}^{-1}$).¹⁷

Electrochemistry is not well suited to the identification and quantification of multiple mixed-solute species, particularly in this case because Si^{IV} is essentially electroinactive, and the speciation proposed by Zhao et al.^{25,26} should not be taken as definitive. ²⁹Si NMR, on the other hand, has identified some 24 small silicate oligomers as well as the monomer in moderately alkaline silicate solutions^{14,18–21} (although the degrees of protonation of the various silicate oligomers are not clearly revealed), and we have therefore chosen this technique, with some consideration of ⁶⁷Zn NMR, to characterize the principal silicate-zincate species present in solutions sufficiently alkaline to give adequate solubilities. High pH is also desirable to limit the plethora of silicate oligomers that may be present to a tractably small number.²¹ By working at temperatures below ambient, the silicate frameworks can be made kinetically inert,²⁷ thus simplifying the interpretation of the silicate-zincate spectra but at the cost of increasing the number of significant oligomers; to offset this, very high alkali concentrations (on the order of 10 mol L^{-1}) have been chosen for optimal results, though this is far from physiological reality. In a similar manner, we used ²⁹Si and ²⁷Al NMR spectroscopy to address the subsidiary question of whether zinc(II) can compete with aluminum(III) for silicate ions in alkaline solution.²⁸ In all cases, the interpretation of the NMR spectra is heavily dependent upon an appreciation of the chemical-exchange kinetics involved.

Experimental Section

House-deionized water was further purified to 18.3 MΩ cm resistivity by passing it through a Barnstead E-pure train.

For preliminary studies of solubility, solutions were prepared using ordinary borosilicate glassware, but polyethylene ware was used for prolonged handling and storage. Zinc metal (Fisher Certified Reagent), ZnCO_3 (Baker Analyzed), ZnCl_2 (Aldrich, 98%), granulated Al metal (Fisher), NaOH pellets (EMD, GR ACS 97%), KOH pellets (EMD, 85%), and fumed silica (Sigma-Aldrich, 99.8%) were used as received. Stock solutions of silicate were prepared by dissolving fumed silica in alkali of the requisite concentration; slight traces of pale brown insoluble matter, if present, were removed by decantation. Stock aluminate solutions were made by dissolving Al granules in aqueous alkali with cooling and decanting the solution from small amounts of black residue. Zincate solutions were made by dissolving ZnCO_3 , ZnCl_2 , or ZnO in alkali. The solubility limits of the silicate-zincate mixtures at room temperature (~ 22 °C) were determined by adding zincate solution dropwise from a buret to an agitated silicate solution until a slight persistent precipitate was observed. Aluminosilicate solubility limits were similarly established. To estimate the solubility of the Si/Zn/Al mixtures, homogeneous silicate-zincate solutions were titrated with aluminate solutions to incipient precipitation. It was possible that

(15) Baes, C. F., Jr.; Mesmer, R. E. *The Hydrolysis of Cations*; Wiley-Interscience: New York, 1976; pp 287–294.

(16) Birchall, J. D.; Bellia, J. P.; Roberts, N. B. *Coord. Chem. Rev.* **1996**, *149*, 231.

(17) Iler, R. K. *The Chemistry of Silica*; Wiley: New York, 1979.

(18) Harris, R. K.; Newman, R. H. *J. Chem. Soc., Faraday Trans. 2* **1977**, *73*, 1204.

(19) Harris, R. K.; Knight, C. T. *J. Chem. Soc., Faraday Trans. 2* **1983**, *79*, 1525.

(20) Harris, R. K.; Knight, C. T. *J. Chem. Soc., Faraday Trans. 2* **1983**, *79*, 1539.

(21) Kinrade, S. D.; Swaddle, T. W. *Inorg. Chem.* **1988**, *27*, 4253.

(22) Nossov, A.; Swaddle, T. W. Unpublished observations.

(23) Hazel, J. F.; McNabb, W. M.; Machermer, P. E. *J. Electrochem. Soc.* **1952**, *99*, 301.

(24) Scheirer, D. E. *An Electrometric Study of the Reactions of Zinc and Cadmium Ions with Sodium Silicates*; Ph.D. Thesis: University of Pennsylvania, Philadelphia, PA, 1953.

(25) Zhao, C.; Huang, S.; Zeng, L. *Human Daxue Xuebao* **1983**, *10*, 1.

(26) Zeng, L.; Zhao, C.; Huang, S.; Chen, B.; Qu, L. *Human Daxue Xuebao* **1985**, *12*, 100.

(27) Vallazza, E.; Bain, A. D.; Swaddle, T. W. *Can. J. Chem.* **1998**, *76*, 183.

(28) North, M. R.; Swaddle, T. W. *Inorg. Chem.* **2000**, *39*, 2661.

some solutions prepared in this way were supersaturated, since many solutions of aluminosilicates prepared in this way have been found to be metastable with lifetimes that vary widely with composition and temperature in complicated ways.²⁹ Accordingly, the longevity of dummy solutions with compositions selected for NMR measurements was always checked by allowing them to stand for at least 15 h.

For NMR spectroscopy, solutions in water (20% D₂O for shimming purposes) were prepared by weight using polyethylene or Teflon-FEP ware. In early experiments using KOH, the pellets of which contained much water and carbonate, concentrations were recorded in mol L⁻¹ and are reported as such here, but for NaOH solutions, the molal scale (moles of solutes per kg solvent) was used. To avoid paramagnetic contaminants, which may be associated in particular with the concentrated alkali and can affect ²⁹Si NMR spectra adversely,²⁷ high purity KOH hydrate pellets (Fluka 60371, or AESAR 99.995% on a metals basis), ZnO (Sigma-Aldrich 99.999%), and Al rod (Spex Industries AL07-50 TMI 10) were used; the latter dissolved in alkali leaving no residue. High purity SiO₂ (Alfa AESAR, 99.999% on a metals basis) dissolved too slowly for quantitative silicate solution preparation, but solutions prepared from fumed silica as above gave essentially identical ²⁹Si NMR spectra. Since the alkali pellets inevitably contained carbonate ions and water, the alkali and carbonate contents of solutions were determined by diluting a weighed aliquot (nominally 1.00 mL) of the solution with water and titrating it potentiometrically with standard HCl (Fisher, 0.1003 mol L⁻¹).

Solution samples were placed in Teflon liners in 10 mm NMR tubes, purged with Ar, and securely stoppered. NMR spectra were taken at the University of Calgary on a Bruker AMX-300 wide-bore spectrometer (7.05 T), with the temperature controlled to ±1 K and calibrated against methanol and ethylene glycol.^{30,31} The chemical shifts, δ , of ²⁹Si were referenced to tetramethylsilane (TMS: $\delta(^{29}\text{Si}) = 59.6$ MHz), those of ²⁷Al to were referenced to 1 mol L⁻¹ aqueous AlCl₃ (78.2 MHz), and those of ⁶⁷Zn were referenced to 1.5 mol L⁻¹ aqueous Zn(ClO₄)₂ (18.76 MHz). For the solutions of interest, ²⁹Si 90° pulse widths (18 μ s, cf. 22 μ s for TMS) and longitudinal relaxation times, T_1 (typically ~5 s), were measured, and the spectra were collected with 600–5500 30° pulses at intervals of 2 T_1 . A blank ²⁹Si spectrum of aqueous alkali was subtracted digitally in each case to eliminate any effects of a broad resonance centered at about -115 ppm from the Si in the NMR tube and coil supports. For ²⁷Al, T_1 was ca. 10 ms, and the spectra were collected with ~1000 90° pulses of 23 μ s at 0.4 s intervals. From each, an ²⁷Al spectrum of an aqueous alkali blank was subtracted to correct for a broad weak resonance centered at 69 ppm from the Al in the probehead. The ⁶⁷Zn spectra were collected with 128 (Zn(ClO₄)₂ standard) or 18 900–150 000 (Zn in alkaline media) 90° pulses of 25.8 μ s at 0.1 s intervals.

Throughout this Article, “line width” means full line width at half the maximum peak height.

Computational Details. Optimized gas-phase geometries were obtained at the HF/6-31G* level using the software packages Gaussian 98 and Gaussian 03.^{32,33} For some of the anions with larger charges, the Si–O, Al–O, and Zn–O bond distances predicted were unusually large, but this is to be expected for gas-phase calculations. Some anions with the largest charges, 7- and 8-, were entirely unstable in the gas-phase even when diffuse functions were added

to the basis set and geometry optimizations were performed with the 6-31+G(d,p) basis set. ²⁹Si NMR shieldings calculated by the gauge including atomic orbital method,³⁴ as implemented in Gaussian 98, were obtained at the *HF/6-311+G(2d,p) level. We have found previously that this computational level yields errors in ²⁹Si shifts, calculated in the gas phase, within 6 ppm for monomeric organosilicate complexes.³⁵ Isotropic shifts (δ) are obtained as the difference between the theoretically predicted shielding for tetramethylsilane (TMS) and the shielding of the relevant molecule. The NMR shieldings were calculated in the gas phase (NMR-1). The effect of solvation on the geometries and shieldings was taken into account via a self-consistent reaction field using the polarizable continuum model of Tomasi and co-workers,³⁶ implemented in the Gaussian programs as the “SCRF=COSMO” keyword. NMR shieldings within the COSMO implementation were obtained for molecules whose geometries were optimized in the gas phase (NMR-2) and for those with geometries optimized within the COSMO SCRF (NMR-3). In some cases, the geometry optimization did not converge, even within the COSMO SCRF solvation method, and for some molecules, the COSMO NMR calculation did not converge on the gas-phase molecules. In these cases, we resorted to NMR-2 or NMR-1 results, respectively, for comparison with the experimental results. NMR-3 (and NMR-2 in cases where NMR-3 results could not be obtained) results are shown in Table 1 in the “calculated, solution” column; NMR-1 results are shown in the “calculated, gas phase” column. In general, the trends obtained were similar, with the error in solution results (2–4 ppm) being smaller than that for the gas-phase results.

Results and Discussion

Solubility Phenomena. Zinc oxide was soluble in ~12 mol L⁻¹ NaOH to the extent of ~1.4 mol L⁻¹ at room temperature. The semiquantitative solubility observations for solutions of ZnO in the presence of SiO₂ in 6.5–10.0 mol L⁻¹ NaOH or KOH can be summarized by saying that homogeneous solutions could be obtained when the condition $[\text{ZnO}] \times [\text{SiO}_2] \approx 0.4 \text{ mol}^2 \text{ L}^{-2}$ (with $[\text{Zn}]/[\text{Si}]$ ranging from 0.12 to 2.0) was not exceeded, although a stable homogeneous solution was also obtained with $[\text{ZnO}] \approx [\text{SiO}_2] \approx 0.85 \text{ mol L}^{-1}$ in 10 mol L⁻¹ KOH. The solutions appeared to be indefinitely stable.

- (29) North, M. R.; Fleischer, M. A.; Swaddle, T. W. *Can. J. Chem.* **2001**, *79*, 75.
 (30) Van Geet, A. L. *Anal. Chem.* **1968**, *40*, 2227.
 (31) Ammann, C.; Meier, P.; Merbach, A. E. *J. Magn. Reson.* **1982**, *46*, 319.
 (32) Frisch, M. J.; Trucks, G. W.; Schlegel, H. B.; Scuseria, G. E.; Robb, M. A.; Cheeseman, J. R.; Zakrzewski, V. G.; Montgomery, J. A., Jr.; Stratmann, R. E.; Burant, J. C.; Dapprich, S.; Millam, J. M.; Daniels, A. D.; Kudin, K. N.; Strain, M. C.; Farkas, O.; Tomasi, J.; Barone, V.; Cossi, M.; Cammi, R.; Mennucci, B.; Pomelli, C.; Adamo, C.; Clifford, S.; Ochterski, J.; Petersson, G. A.; Ayala, P. Y.; Cui, Q.; Morokuma, K.; Malick, D. K.; Rabuck, A. D.; Raghavachari, K.; Foresman, J. B.; Cioslowski, J.; Ortiz, J. V.; Stefanov, B. B.; Liu, G.; Liashenko, A.; Piskorz, P.; Komaromi, I.; Gomperts, R.; Martin, R. L.; Fox, D. J.; Keith, T.; Al-Laham, M. A.; Peng, C. Y.; Nanayakkara, A.; Gonzalez, C.; Challacombe, M.; Gill, P. M. W.; Johnson, B. G.; Chen, W.; Wong, M. W.; Andres, J. L.; Head-Gordon, M.; Replogle, E. S.; Pople, J. A. *Gaussian 98*; Gaussian, Inc.: Pittsburgh, PA, 1998.
 (33) Hehre, W. J.; Radom, L.; Schleyer, P. v. R.; Pople, J. A. *Ab Initio Molecular Orbital Theory*; Wiley: New York, 1986.
 (34) Wolinski, K.; Hinton, J. F.; Pulay, P. *J. Am. Chem. Soc.* **1992**, *112*, 8251.
 (35) Sahai, N. *Geochim. Cosmochim. Acta* **2004**, *68*, 227.
 (36) (a) Miertus, S.; Scorocco, E.; Tomasi, J. *J. Chem. Phys.* **1981**, *55*, 117. (b) Barone, V.; Cossi, M.; Tomasi, J. *J. Chem. Phys.* **1997**, *107*, 3210. (c) Mennucci, B.; Cancès, E.; Tomasi, J. *J. Phys. Chem. B* **1997**, *101*, 10506. (d) Amovilli, C.; Barone, V.; Cammi, R.; Cancès, E.; Cossi, M.; Mennucci, B.; Pomelli, C. S.; Tomasi, J. *Adv. Quantum Chem.* **1998**, *32*, 227. (e) Cossi, M.; Scalmani, G.; Rega, N.; Barone, V. *J. Chem. Phys.* **2002**, *117*, 43.

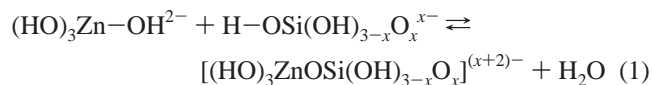
Table 1. Calculated and Observed ^{29}Si Chemical Shifts for Complexes of Silicate Anions with Zincate, Aluminate, or Both in Aqueous Solution

	formula	$\delta(^{29}\text{Si})$ (ppm) ^a		
		calculated, solution ^b	calculated, gas phase ^c	observed ^d
A	$\text{Si}(\text{OH})_4$	-71	-70	
B	$[\text{Si}(\text{OH})_3\text{O}]^-$	-71	-68	
C	$[\text{Si}(\text{OH})_2\text{O}_2]^{2-}$	-68	-66	-72.1 (1-1); -71.3 ^{e,f}
D	$[\text{Si}(\text{OH})\text{O}_3]^{3-}$	-64	-58	
E	$[\text{SiO}_4]^{4-}$	-63	-56	
F	$[(\text{HO})_3\text{SiOSi}(\text{OH})_3]$	-79	-83	
G	$[(\text{O}(\text{HO})_2\text{SiOSi}(\text{OH})_2\text{O})]^{2-}$	-79 ^g	-86	
H	$[\text{O}_2(\text{HO})\text{SiOSi}(\text{OH})\text{O}_2]^{4-}$	-73	-75	-78.9 (1-2); -78.6 ^f
I	$[\text{O}_3\text{SiOSiO}_3]^{6-}$	-74 ^h	-66	
J	$[(\text{HO})_3\text{ZnOSiO}_2\text{OH}]^{4-}$	-69 ^g	-68	-71.4 (1-12)
K	$[(\text{HO})_3\text{ZnO}(\text{SiO}_2)\text{O}(\text{SiO}_2)\text{OH}]^{6-}$	-77, -74 ^g	-77, -76	-76.4 (1-13)
L	$[(\text{HO})_3\text{AlOSiO}_2\text{OH}]^{3-}$	-72	-72	-75.0 (2-4)
M	$[(\text{HO})_3\text{ZnO}(\text{SiO}_2)\text{OAl}(\text{OH})_3]^{5-}$	-67	-72	
N	$[\text{O}_2(\text{HO})\text{SiO}(\text{SiO}_2)\text{OSi}(\text{OH})\text{O}_2]^{6-}$	-75, ^{g,i} -86 ^{g,j}	-77, ⁱ -87 ^j	-78.2, -86.4 ^f
O	cyclic $[\{(\text{HO})_2\text{SiO}\}_3]^{9-}$	-87 ^g	-89	
P	cyclic $[\{(\text{HO})\text{OSiO}\}_3]^{3-}$	-82 ^g	-82	
Q	cyclic $[(\text{O}_2\text{SiO}_3)]^{6-}$	-78 ^g	-78	-81.6 (1-3); -81.5; ^e -81.0 ^f
R	$[\text{O}_2(\text{HO})\text{Si}\{(\text{SiO}_3)_3\}]^{7-k}$	-76, ^{g,i} -79, ^{g,j} -91 ^{g,l}	-77, ⁱ -79, ^j -92 ^l	-78.6, -81.4, -88.6 ^{e,f}
S	$[(\text{HO})_3\text{Zn}\{(\text{SiO}_3)_3\}]^{7-m}$	-79, ^{g,j} -82 ^{g,l}	-79, ^j -84 ^l	-76.8 (1-9, 1-14), -82.6 (1-11, 1-16)
T	$[(\text{HO})_3\text{ZnO}(\text{SiO}_2)\text{O}(\text{SiO}_2)\text{OZn}(\text{OH})_3]^{8-n}$			
U	$[(\text{HO})_3\text{ZnO}(\text{SiO}_2)\text{O}(\text{SiO}_2)\text{OAl}(\text{OH})_3]^{7-n}$			
V	$[(\text{HO})_3\text{ZnO}(\text{SiO}_2)\text{O}(\text{SiO}_2)\text{O}(\text{SiO}_2)\text{OH}]^{8-n}$			
W	$[(\text{HO})_3\text{ZnO}(\text{SiO}(\text{OH}))\text{O}(\text{SiO}(\text{OH}))\text{O}(\text{SiO}_2)\text{OH}]^{6-}$	-83, -83 ^g	-84, -84	

^a Relative to $\text{Si}(\text{CH}_3)_4$ (TMS, calculated chemical shielding = 386.0 ppm in both the gas phase and in the COSMO model of solvation); chemical shifts are calculated at the HF/6-311+G(2d,p) level. ^b NMR-3 results (see Computational Details for explanation). ^c NMR-1 results (see Computational Details for explanation). ^d In aqueous alkali; conditions as in Figures 1 and 2, except as noted. ^e Ref 21; $[\text{NaOH}] = [\text{Si}^{\text{IV}}] = 1.8 \text{ mol kg}^{-1}$, at 269 K. ^f Figure S1 (Supporting Information), 1.69 mol L⁻¹ SiO₂ in 6.4 mol L⁻¹ KOH, with assignments by Harris et al.¹⁸⁻²⁰ ^g NMR-2 results (see Computational Details for explanation). ^h At nonoptimized geometry. ⁱ Terminal Si (Q¹). ^j Bridging Si (Q²). ^k Cyclic trimer with monosilicate side-group. ^l Bridgehead Si (Q³). ^m Cyclic trimer with zincate side group. ⁿ Calculations show this anion to be unstable.

Solutions of aluminate in the presence of silicate, however, are usually metastable. In a previous study,²⁹ it was shown that the lifetimes of homogeneous solutions of silicate with aluminate are generally longest when the alkali concentration, the ratio $[\text{Si}]/[\text{Al}]$, or both are high, although long-lived solutions can also be prepared at somewhat lower alkalinities when $[\text{Si}] \approx [\text{Al}]$. In the present work, cases in which $[\text{Al}] \gg [\text{Si}]$ were also examined, and it was found that homogeneous solutions could be made in 15 mol L⁻¹ NaOH with, for example, $[\text{Al}] \approx 1.7 \text{ mol L}^{-1}$ and $[\text{Si}]$ up to about 0.05 mol L⁻¹, although precipitation set in after about 3 weeks for this concentration of silicate or immediately if more silicate solution were added.

Precipitation occurred quickly when an aluminate solution was added to Zn–Si solutions in KOH media but not in NaOH solutions. An important observation was that zincate greatly increased the tolerance of silicate for aluminate in the NaOH media. Thus, solutions of 0.5 mol L⁻¹ SiO₂ in 15 mol L⁻¹ NaOH gave clear solutions with concentrations of both Zn and Al varying between 0.3 and 0.8 mol L⁻¹, with no indication of precipitation after more than 3 weeks. Since zincate and aluminate appear not to interact significantly with each other (see discussion of ²⁷Al spectra, below), this implies either that zincate scavenges free silicate



suppressing the formation and precipitation of aluminosilicates or that soluble ternary zincate–aluminate–silicate

complexes form (or both). We show below that the first explanation is the more plausible.

Silicate–Zincate Interactions: ²⁹Si Spectra. The systematic selection of solute concentrations was sometimes frustrated by solubility limitations; in particular, the choice of alkali was limited to NaOH for all experiments involving Al (see below) and those intended for comparison with Si–Zn–Al systems. Figure 1, however, shows the effect of Zn^{II} (present as $\text{Zn}(\text{OH})_4^{2-}$ at the pH of our solutions¹⁵) on ²⁹Si spectra at 280 K in early experiments in which SiO₂ and ZnO were dissolved in 10.0 mol L⁻¹ aqueous KOH (20% D₂O, 0.28 mol L⁻¹ K₂CO₃, density = 1.442 g cm⁻³, $[\text{KOH}] = 11.5 \text{ mol kg}^{-1}$) for comparison with previous kinetic studies.²⁷ Similar results were obtained when ZnCO₃ was used in place of ZnO and when K₂CO₃ was added; thus, the effects of adventitious carbonate can be neglected. Subsequent experiments using 15.0 mol kg⁻¹ NaOH gave spectra similar to Figure 1, although with reduced silicate oligomer intensities (expected because of the higher alkalinity) and $\delta(^{29}\text{Si})$ 1–2 ppm more positive; thus, the identity of the cation is inconsequential except with respect to solubility and solution longevity.²⁹

In Figure 1, for which $[\text{KOH}]_{\text{total}}$ was 10.0 mol L⁻¹ (11.5 mol kg⁻¹) at 280 K, the top spectrum shows three strong ²⁹Si resonances known¹⁸⁻²¹ to be from the monomer $(\text{HO})_2\text{SiO}_2^{2-}$ (peak 1-1, $\delta(^{29}\text{Si}) = -72.1 \text{ ppm}$, 75% of total Si according to the integrated resonance intensities), dimer $[\text{O}_2(\text{HO})\text{SiOSi}(\text{OH})\text{O}_2]^{4-}$ (1-2, -78.9 ppm, 16%), and cyclic trimer $[(\text{SiO}_3)_3]^{6-}$ (1-3, -81.6 ppm, 8%). For $\text{Si}(\text{OH})_4$, the first and second pK_a values are approximately 9.7 and 12.7, respectively; the third is too large to measure ($\gg 15$), and

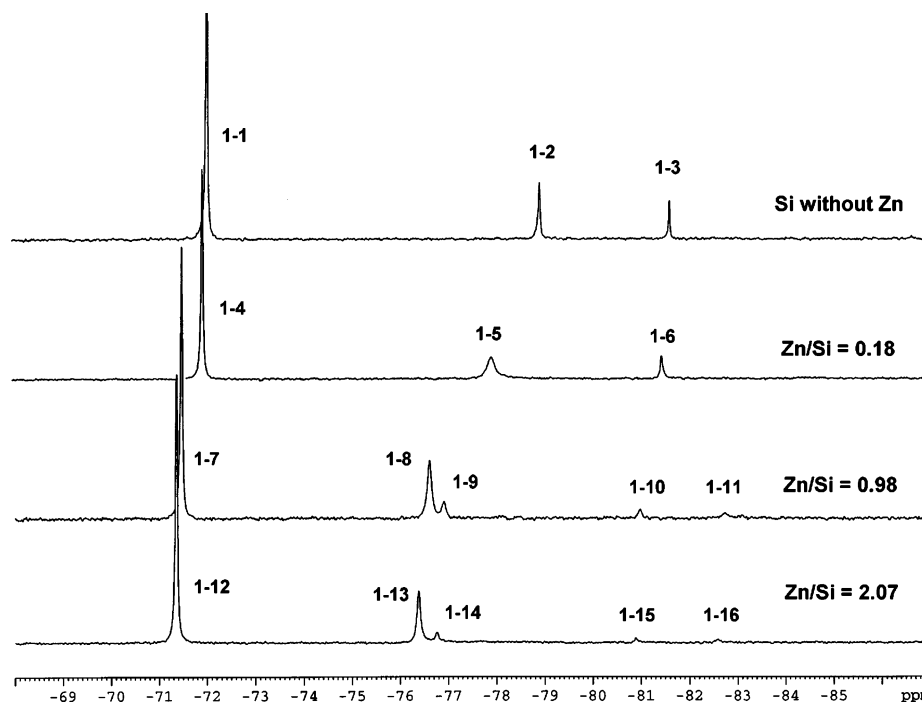


Figure 1. ^{29}Si NMR spectra showing the effect of added ZnO on silicate ions in aqueous KOH (10 mol L $^{-1}$, 20% D $_2$ O) at 280 K. $[\text{Si}]_{\text{total}}$ (from top) = 0.88, 1.33, 0.86, and 0.48 mol L $^{-1}$. Free $[\text{OH}^-]$ (from top) = 8.2, 6.9, 6.6, and 7.1 mol L $^{-1}$. Artificial line broadening = 1 Hz. Probe background has been subtracted. Vertical scales are arbitrary (not the same for all spectra).

the oligomers are generally more acidic than the monomers.¹⁷ The degree of deprotonation, x , for each Si center and hence the negative charge carried by each Q 0 , Q 1 , and Q 2 SiO $_4$ unit³⁷ (cf. Equation 1) may therefore be taken to be 2 for all silicate species in the work described here.³⁸ On this basis, one can calculate pHs of 14.9 for the top spectrum in Figure 1 and 14.8 for the lower three. Because proton exchange on silicate species is rapid, only a single ^{29}Si resonance would be seen even if two or more protonated forms of a given silicate species were present. The rate of Si–Si site exchange between the aqueous silicate species, however, is slow enough to be generally negligible on the ^{29}Si NMR time scale in the 280–315 K range of our experiments.²⁷

Traces of other oligomers account for the remaining 1% of the Si. A spectrum with lower $[\text{KOH}]$ and consequently more detectable oligomers (Figure S1, Supporting Information; cf. Harris and Newman¹⁸) shows that this small fraction consists mostly of the “linear” (acyclic) trimer $[\text{O}_2(\text{HO})\text{SiO}(\text{SiO}_2)\text{OSi}(\text{OH})\text{O}_2]^{6-}$ (species **N** in Table 1), which is in unfavorable equilibrium (slow on the ^{29}Si NMR time scale) with the cyclic trimer,²⁷ and a somewhat lesser amount of a tetramer in which a monosilicate side-group is attached to a

cyclic trimer ring (species **R** in Table 1).^{18–20} For the same solutions at 298 and 315 K, the $\delta(^{29}\text{Si})$ values for the monomer were -72.0 and -71.9 ppm, and for the dimer, they were -78.8 and -78.7 , respectively; therefore, the effect of increasing temperature on the primary silicate resonances is only a very small upfrequency shift. The narrowness (~ 2 Hz) and negligible temperature dependence of the line widths of all three silicate species in 10 mol L $^{-1}$ KOH and 15 mol kg $^{-1}$ NaOH shows that the effect of solution viscosity on ^{29}Si relaxation is negligible.

The effect of Zn $^{\text{II}}$ on the ^{29}Si spectra of the silicate anions in Figure 1 is most clearly seen in the case of the silicate dimer resonance (**1-2**, -78.9 ppm), which is shifted progressively upfrequency (**1-5**, -78.0 ppm; **1-8**, -76.6 ppm) as ZnO is added, reaching a limit (**1-13**, -76.4 ppm) by the point where the stoichiometric $[\text{Zn}]/[\text{Si}]$ ratio exceeds 2. This indicates clearly that zincate is forming a complex with the silicate dimer and, since only a single resonance is seen after addition of Zn $^{\text{II}}$, leaving no trace of the original dimer peak at -78.9 ppm, that the exchange of the dimer with its Zn $^{\text{II}}$ complex is in the fast exchange limit on the ^{29}Si NMR time scale. The latter observation is consistent with the known high lability of Zn $^{\text{II}}$ complexes.³⁹ Because peak **1-5**, for which the stoichiometric $[\text{Zn}]/[\text{Si}]$ ratio is 18%, occurs 0.9 ppm up frequency from the original silicate dimer peak (that is, at 36% of the maximum shift of +2.5 ppm), it follows that the maximum ratio of Zn atoms to Si in the complex is 1:2 (one Zn per silicate dimer). As noted above, there will be a charge of 2– per Si center at pH ≥ 14 , so that the only significant Zn complex formed from the dimer under these conditions

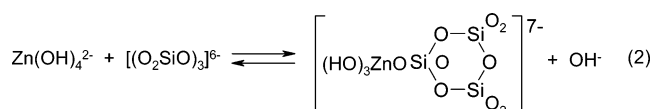
(37) In the established nomenclature, Q n indicates a Si center connected via O to n other nearest-neighbor Si atoms.

(38) In the absence of definitive pK $_a$ values for oligomeric silicates, support for these assertions may be drawn by analogy with linear polyphosphoric acids, in which the only weakly acidic protons are located on the terminal phosphate units and are themselves more acidic than those in monomeric phosphates, while cyclic phosphates behave as anions of strong acids. For example, see: (a) Van Wazer, J. R.; Holst, K. A. *J. Am. Chem. Soc.* **1950**, *72*, 639. (b) *Stability Constants of Metal-Ion Complexes*; Special Publication No. 17; The Chemical Society: London, 1964; pp. 180–201. (c) Greenfield, S.; Clift, M. *The Analytical Chemistry of the Condensed Phosphates*; Pergamon Press: New York, 1975; Chapter 3.

(39) Richens, D. T. *The Chemistry of Aqua Ions*; Wiley: New York, 1997; pp 546–550.

is $[(\text{HO})_3\text{ZnO}(\text{SiO}_2)\text{O}(\text{SiO}_2)\text{OH}]^{6-}$. Because Zn^{II} exchange is very fast, only a single ^{29}Si resonance is seen.

In contrast, the cyclic trimer silicate peak (**1-3**, -81.6 ppm) is only slightly shifted by addition of Zn^{II} to the extent $[\text{Zn}]/[\text{Si}] = 0.18$ (**1-6**, -81.5 ppm), but its intensity becomes progressively reduced as more Zn^{II} is added (**1-10**, -81.1 ppm; **1-15**, -80.9 ppm), while new features appear at -76.8 ppm (**1-9**, **1-14**) and with lower intensity, -82.6 ppm (**1-11**, **1-16**). Since the development of the new features is in step with the disappearance of the cyclic trimer peak, it may be ascribed to the formation of a $[(\text{HO})_3\text{Zn}\{(\text{SiO}_3)_3\}]^{7-}$ complex (species **S** in Table 1) between a zincate ion and the cyclic trimer. The complex has one proximal Si (**1-11**, **1-16**) for every two distal Si atoms (**1-9**, **1-14**) in the silicate ring, so accounting roughly for the difference in peak intensities.



Because the cyclic trimer $[(\text{O}_2\text{SiO})_3]^{6-}$ (species **Q**) has no $\text{HO}-\text{Si}\equiv$ groups available for a facile condensation reaction (cf. eq 1), this process will be much slower than (e.g.) the reaction of zincate with $[\text{O}_2(\text{HO})\text{SiOSi}(\text{OH})\text{O}_2]^{4-}$, as discussed above. In the slow exchange limit, the cyclic trimer ^{29}Si resonance would be slightly broadened by any chemical exchange but its frequency would not be detectably affected. If the exchange is somewhat faster, the peaks will be substantially broadened because of incipient coalescence and also shifted toward the coalescence frequency, which may be calculated from the bottom two spectra of Figure 1 to be about -79.7 ppm. In fact, the cyclic trimer peak moves from -81.6 ppm (**1-3**) to -81.4 (**1-6**), -81.0 (**1-10**), and -80.9 ppm (**1-15**), with line widths of 0.8, 2.5, 4.2, and 5.6 Hz, respectively, at 280 K, as Zn^{II} is added up to $\text{Zn}/\text{Si} = 2.07$ (line widths for species **S** were not satisfactorily measurable). Thus, it appears that slow exchange between species **Q** and **S** does occur, causing moderate broadening of the ^{29}Si resonance of **Q**, but may be too slow to account for the 0.7 ppm up frequency displacement of the cyclic trimer resonance as Zn^{II} is added. In any event, the coalescence of the **Q** and **S** resonances is unlikely to be closely approached because the concentrations of **Q** and **S** become small at high zincate concentrations.

A second possible interpretation of the effect of Zn^{II} on the cyclic trimer resonance is that addition of zincate occurs rapidly to a terminal silicate unit of the acyclic silicate trimer **N** (visible at -86.4 and -78.2 ppm in Figure S1 but lost in the baseline noise of Figure 1) with which the cyclic trimer is known to be in equilibrium on the time scale of sample preparation.²⁷ The ring-opening process, however, is too slow (extrapolated rate constant $9 \times 10^{-5} \text{ s}^{-1}$ at 280 K)²⁷ to allow this process to proceed at a significant rate. Moreover, theoretical calculations imply that the hypothetical Zn^{II} -acyclic trimer complex, **V** (Table 1), would be electrostatically unstable (see below).

A third alternative explanation for the 0.7 ppm up frequency displacement of the cyclic trimer resonance as Zn^{II} is added is that it is the result of an unidentified general medium effect of zincate that affects all Si nuclei similarly. This interpretation gains credibility from the fact that the silicate monomer resonance shows a parallel upfrequency displacement of 0.6–0.7 ppm (peaks **1-1**, **1-4**, **1-7**, and **1-11**). This alternative is considered further below.

Figure 1 shows a surprisingly small (0.6–0.7 ppm up frequency) change in the chemical shift $\delta(^{29}\text{Si})$ of the monomer peak upon addition of Zn^{II} . This might be attributed to some general medium effect induced by zincate, particularly since the cyclic trimer resonance shows a parallel shift, but the fact that the increase shows saturation near $\text{Zn}/\text{Si} = 1$ (**1-7**, cf. **1-12**) points instead to a 1:1 interaction of the silicate monomer with the zincate ion. Similar experiments with 15.0 mol kg^{-1} NaOH confirm the saturation of the monomer shift effect at $\text{Zn}/\text{Si} \geq 1$. The broadening of the monomer resonance upon the addition of Zn^{II} (line widths 1.3, 1.6, 1.8, and 2.1 Hz for peaks **1-1**, **1-4**, **1-7**, and **1-12**, respectively, at 280 K) is much less than that for the cyclic trimer, suggesting that the effects of zincate on the silicate monomer and cyclic trimer may not be directly comparable. Since the solubility of silicates (present largely as the monomer) in the presence of aluminate is strongly enhanced by addition of Zn^{II} , it can be inferred that zincate interacts chemically with the silicate monomer. Moreover, given the clear evidence for a strong 1:1 specific interaction between zincate and the silicate dimer, it can be confidently expected that a similar interaction occurs between Zn^{II} and the monomer. Thus, it may be concluded that peaks **1-1**, **1-4**, **1-7**, and **1-12** represent the progressive formation of a 1:1 complex between zincate and monomeric silicate, albeit with $\delta(^{29}\text{Si})$ only 0.6–0.7 ppm more positive than that for the silicate monomer in the limiting case (stoichiometric $[\text{Zn}]/[\text{Si}] = 2.07$). For stoichiometric $[\text{Zn}]/[\text{Si}] = 0.18$ (peak **1-4**), the shift is about +0.1 ppm, consistent with the formation of a 1:1 complex. Furthermore, since the feature **1-4** is a single narrow line, rather than separate resonances corresponding to the monomeric silicate and the proposed Zn–Si species, the exchange of ^{29}Si between this complex and the free monomeric silicate must be very fast on the ^{29}Si NMR time scale, as expected in view of the high-substitutional lability of simple zinc(II) complexes.³⁹

If we disregard the saturation effect at $\text{Zn}/\text{Si} \approx 1$, it may be argued that the 0.6–0.7 ppm displacement of the monomeric silicate resonance upon the addition of zincate could be mainly the result of the general medium effect considered above for the cyclic trimer and that the contribution of complex formation to this displacement may be small or zero; be this as it may, the salient point is that the effect of complexation by zincate on $\delta(^{29}\text{Si})$ for monomeric silicate is very small. A comparison of the $\delta(^{29}\text{Si})$ values for cyclic species **Q** and **S** also shows only a small down frequency (-1 ppm) displacement for the Si center to which zincate is attached but a large up frequency (+5 ppm) shift for the distal Si nuclei. On this basis, we may expect that the change in $\delta(^{29}\text{Si})$ following the addition of zincate to one end of

the silicate dimer should again be 0 ± 1 ppm and around +5 ppm for the proximal and distal Si nuclei, respectively, but, because the exchange of Zn^{II} between the two Si centers is fast on the NMR time scale, an averaged $\delta(^{29}\text{Si})$ of about +2.5 ppm should result from complex formation. This is indeed the case (compare $\delta(^{29}\text{Si})$ for **1-13** with **1-2**, Table 1).

It might be argued that the small change in $\delta(^{29}\text{Si})$ for the monomeric silicate upon addition of ZnO is the result of partial reprotonation of the silicate monomer following the reduction of the pH upon dissolution of the ZnO, but $\delta(^{29}\text{Si})$ does not follow the concentration of free OH^- , which in any case remains high enough to keep all of the monomer in the $(\text{HO})_2\text{SiO}_2^{2-}$ form. Besides, as the theoretical calculations presented in Table 1 confirm, the effect of protonation is to make $\delta(^{29}\text{Si})$ more negative.

The integrated ^{29}Si intensities of peaks **1-1**, **1-4**, **1-7**, and **1-12** (monomeric silicate and its monozincate complex) correspond to 75, 62, 60, and 69%, respectively, of the total silicon at 280 K, with similar distributions at 298 and 315 K. This is consistent with the inference that complex formation by zincate can consume two Si atoms per Zn as the dimeric silicate (forming species **K**) but only one Si per Zn as the monomer, shifting the equilibrium Si distribution away from the monomeric silicate. At the same time, the cyclic trimer $[\text{Si}_3\text{O}_9]^{6-}$, although prominent in the absence of Zn, almost disappears, partly through the formation of the species **S** but also through dispersal into the silicate pool in response to scavenging of the monomer and dimer by zincate. It is not possible to extract the formation constants for the various silicate–zincate complexes from the NMR spectra because of the number of species present, but the integrated intensity data suggest that zincate forms complexes with the silicate dimer preferentially over the monomer. The partial recovery of the percentage of monomeric silicate (as its zincate complex) on going to excess Zn probably reflects the reduction of the contributions of the cyclic trimer and any trace amounts of higher oligomers to the total Si.

Finally, we note that spectra corresponding to Figure 1 taken at 280, 298, and 315 K show only very minor differences. As the temperature increases, the exchange between the all-silicate species remains in the slow limit, while the exchange of Zn (already in the fast exchange regime) becomes even faster so that the ^{29}Si resonances become slightly sharper.

Theoretical Calculation of ^{29}Si Chemical Shifts. Because the change in $\delta(^{29}\text{Si})$ between **1-1** and **1-12** as zincate is added is disappointingly small and the assignments of peaks **1-9/14** and **1-11/16** are somewhat tentative, theoretical calculations of $\delta(^{29}\text{Si})$ were made to provide guidance as to the changes to be expected when the proton in a $\equiv\text{Si}-\text{O}-\text{H}$ function is ionized away or replaced by $-\text{SiO}_x(\text{OH})_{3-x}^{x-}$, $-\text{Zn}(\text{OH})_3^-$, or $-\text{Al}(\text{OH})_3$ (at the pH of our experiments, neither $\text{Zn}(\text{OH})_4^{2-}$ nor $\text{Al}(\text{OH})_4^-$ undergoes deprotonation,^{14,15,39,40} unlike the much more acidic $\text{Si}(\text{OH})_4$ ¹⁷). The theoretical $\delta(^{29}\text{Si})$ values summarized in Table 1 for aqueous

species using the NMR-2 and NMR-3 procedures are not very different from those calculated for the gas phase by NMR-1 but nevertheless should not be expected to match the experimental $\delta(^{29}\text{Si})$ closely, especially for the silicate monomers which are surrounded on all sides by hydrogen bonds to solvent and possibly counterions (K^+ or Na^+).⁴¹ The inherent uncertainty in the calculated $\delta(^{29}\text{Si})$ values is around 2–3 ppm.

Our computational results in Table 1 indicate that deprotonation of $\equiv\text{Si}-\text{O}-\text{H}$ centers in species **A–E**, **F–I**, and **O–Q** results in up frequency shifts in $\delta(^{29}\text{Si})$ averaging 2–3 ppm per proton. The $\delta(^{29}\text{Si})$ values from the NMR-2 and –3 calculations are consistently 3 ± 1 ppm more negative than the corresponding experimental $\delta(^{29}\text{Si})$ values in solution. The benchmark for this is species **C**, which is known to be the dinegative monomer anion as shown above. The effect is probably a systematic error originating in the large shielding (386 ppm) calculated for the TMS reference.

The effects of Zn^{II} and Al^{III} on silicate speciation can be seen by comparing the results for species **H**, **L**, and **J** with those of **C**. The replacement of H^+ in a $\equiv\text{Si}-\text{O}-\text{H}$ function by $-\text{SiO}_2(\text{OH})^-$, $-\text{Al}(\text{OH})_3$, and $-\text{Zn}(\text{OH})_3^-$ results in changes in the theoretical $\delta(^{29}\text{Si})$ of about –7, –4, and –1 ppm, respectively. The observed changes are –7, –4, and +0.6 ppm. Given the inherent uncertainty of 2–3 ppm in the calculations, this explains the smallness of the effect (+0.6 ppm) when zincate interacts with monomeric silicate. The predicted shifts for species **K** are consistent with the assignment of peaks **1-8** and **1-13** to $[(\text{HO})_3\text{ZnO}(\text{SiO}_2)-\text{O}(\text{SiO}_2)\text{OH}]^{6-}$, if one keeps in mind that, in the experimental case, the two Si sites are indistinguishable because of the rapid exchange of zincate.

Computations of $\delta(^{29}\text{Si})$ for the highly charged species **T**, **U**, and **V** could not be completed because the geometry optimizations failed to converge, either in the gas phase or when solvation was taken into account. These computational results imply that highly charged species, such as **T**, **U**, and **V**, are electrostatically unstable both in the gas phase and in aqueous solution. This explains why the reaction of zincate with the silicate dimer goes no further than $[(\text{HO})_3\text{ZnO}(\text{SiO}_2)-\text{O}(\text{SiO}_2)\text{OH}]^{6-}$, and it also makes it very unlikely that both zincate and aluminate could be attached simultaneously to the silicate dimer (species **U**). More generally, the increase in the number of detectable silicate oligomers in alkaline silicate solutions as the pH is reduced²¹ can be attributed to the stabilization of the larger anions by reducing their negative charge through protonation of $\equiv\text{Si}-\text{O}-$ functions (compare the calculations for species **V** and **W**).

Furthermore, the predicted shifts for species **S** confirm that the weak peaks **1-9/14** and **1-11/16**, which are associated with the disappearance of the cyclic trimer, can be confidently attributed to the attachment of zincate to one oxygen of the cyclic trimer (cf. the known species **R**) as in eq 2. The failure of calculations for species **V** affirms that the alternative interpretation given above (attachment of zincate

(40) Akitt, J. W. *Prog. Nucl. Magn. Reson. Spectrosc.* **1989**, *21*, 1.

(41) Moravetski, V.; Hill, J.-R.; Eichler, U.; Cheetham, A. K.; Sauer, L. *J. Am. Chem. Soc.* **1996**, *118*, 13015.

to one end of the acyclic trimer anion following ring opening of species **Q**) can be rejected.

Ion Pairing. One possible complication in the interpretation of the NMR spectra of the various anions is that ion pairing with K^+ or Na^+ may influence $\delta(^{29}Si)$.⁴¹ Fuoss-type calculations⁴² for the formation constant for the aqueous ion pair $\{[(HO)_2SiO_2]^{2-}, K^+\}$, assuming radii of 240 and 138 pm for the *unhydrated* silicate and K^+ ions, give 6.0 and 0.29 L mol⁻¹ at ionic strengths of 0 and 10 mol L⁻¹, respectively, at 298 K, meaning that up to 75% of the monosilicate could be ion-paired in 10 mol L⁻¹ KOH (if cation hydration is retained in an ion pair, the fraction of ion pairs will be substantially less). Theoretical calculations show that, in the gas phase, $\delta(^{29}Si)$ for the ion pair (in which Na^+ is in bidentate coordination) may be 4.4 ppm more positive than for $(HO)_2SiO_2^{2-}$, the main component of silicate solutions in concentrated NaOH. The experimental value of $\delta(^{29}Si)$ for $(HO)_2SiO_2^{2-}$, however, is 4 ppm more *negative* than that calculated for aqueous solution by the NMR-3 procedure. It may therefore be concluded that ion pairing is not a major complicating factor in the foregoing interpretations of ²⁹Si spectra.

Silicate–Zincate Interactions: ⁶⁷Zn Spectra. The quadrupolar ⁶⁷Zn nucleus has low receptivity and gives notoriously broad NMR spectra in solution in all but the most symmetrical environments, such as $Zn(H_2O)_6^{2+}$.^{43–47} The reference solution, 1.5 mol L⁻¹ $Zn(ClO_4)_2$ in 20% D₂O ($\delta(^{67}Zn) = 0$), gave a line width of 46 Hz at 280 K, but 0.63 mol L⁻¹ $Zn(OH)_4^{2-}$ in 10.0 mol L⁻¹ KOH at 280 K gave a single peak at $\delta(^{67}Zn) = +220$ ppm with line width of 554 Hz, suggesting either that the symmetry of the Zn^{II} site in this anion is far from the commonly supposed T_d or that solution viscosity or hydrogen bonding between zincate and solvent water cause the line broadening. Cain et al.⁴⁷ suggest that polynuclear aggregation of zincate in highly alkaline solution (albeit at $[Zn^{II}]$ somewhat higher than ours) might also contribute to the large ⁶⁷Zn line width through the effect of increased molecular mass on T_1 . When 0.84 mol L⁻¹ ZnO and 0.86 mol L⁻¹ SiO₂ were dissolved in 10.0 mol L⁻¹ KOH, the line width of the ⁶⁷Zn resonance centered at $\sim +286$ ppm was in excess of 2500 Hz, consistent with strong silicate–zincate interactions. In comparison, for 0.98 mol L⁻¹ ZnO and 0.48 mol L⁻¹ SiO₂ dissolved in 10.0 mol L⁻¹ KOH, the line width was ~ 1360 Hz at $\delta(^{67}Zn) = 240$ ppm; the halving of the line width and the shift toward the zincate frequency can be attributed to averaging through very rapid ⁶⁷Zn exchange⁴⁶ between roughly equimolar amounts of free zincate and $[(HO)_3ZnOSiO_2OH]^{4-}$. These data, crude though they are, confirm that an excess of zincate over silicate does *not* lead to formation of species with more than one Zn^{II} per Si^{IV}.

(42) Fuoss, R. M. *J. Am. Chem. Soc.* **1958**, *80*, 5059.

(43) Epperlein, B. W.; Krüger, H.; Lutz, O.; Schwenk, A. *Z. Naturforsch.* **1974**, *29a*, 1553.

(44) Maciel, G. E.; Simeral, L.; Ackerman, J. J. H. *J. Phys. Chem.* **1977**, *81*, 263.

(45) Li, Z.-f.; Popov, A. I. *J. Solution Chem.* **1982**, *11*, 17.

(46) Epeville, A.; Detellier, C. *Can. J. Chem.* **1986**, *64*, 1845.

(47) Cain, K. J.; Melendres, C. A.; Maroni, V. A. *J. Electrochem. Soc.* **1987**, *134*, 519.

Table 2. Chemical Shifts and Line Widths of ²⁷Al Resonances in 15.0 mol kg⁻¹ NaOH at 298 K^a

sample	[Al ^{III}] (mol kg ⁻¹)	[Si ^{IV}] (mol kg ⁻¹)	[Zn ^{II}] (mol kg ⁻¹)	$\delta(^{27}Al)$ (ppm) ^b	line width (Hz)
A	0.56			76.2	726
B	1.61	0.065		77.7	1500
C	0.57		0.57	76.7	795
D	0.58	0.30	0.58	76.7	890
E	0.58	0.59	0.61	76.3	981

^a As in Figure S2 (Supporting Information). ^b Relative to $\delta(^{27}Al) = 0$ for 0.56 mol L⁻¹ aqueous AlCl₃.

Attempts to reduce the ⁶⁷Zn line widths through working at temperatures higher than 280 K⁴³ produced no significant improvements.

Silicate–Zincate–Aluminate Interactions: ²⁷Al Spectra. ²⁷Al spectra of solutions of Al^{III} in 15.0 mol kg⁻¹ NaOH (20% D₂O), with or without added SiO₂ and ZnO, were taken at 298 K. Baseline corrections for Al in the probehead were subtracted but were unimportant. Single symmetrical lines were observed in all cases, and their characteristics are summarized in Table 2 and Figure S2 (Supporting Information). Zincate as such (spectrum C) has very little effect ($\sim 10\%$ line broadening) on the aluminate resonance, implying that any zincate–aluminate interactions are of minor importance and can be neglected. In contrast, even a relatively small concentration of silicate produced a large ²⁷Al line broadening (spectrum B). The small silicate concentration in the Al–Si sample was the maximum possible in the presence of aluminate (even so, the solution was probably metastable), but a much higher silicate concentration was tolerated when zincate was also present (spectra D and E), either because zincate depletes the silicate pool or because freely soluble Al–Si–Zn species form. The former explanation is the more credible because the ²⁷Al line widths when Al, Si, and Zn are all present are only slightly larger than when Si is absent.

In previous studies of aluminate–silicate interactions,^{28,48} the inverse solubility-limited situation ($[Al^{III}] \ll [Si^{IV}]$) was investigated, and some structure attributable to various degrees of Al–Si connectivity was seen in the ²⁷Al signal. It was also shown, however, that the usually very slow Si–Si exchange rates were increased by about 4 orders of magnitude by complexation with aluminate. In the present study, much free aluminate is present in the Al–Si solution, resulting in rapid exchange with the aluminosilicate species present and, consequently, broad featureless ²⁷Al resonances.

Silicate–Zincate–Aluminate Interactions: ²⁹Si Spectra. Figure 2 shows the effect of adding aluminate and zincate, first separately and then together, to solutions of silicate in 15.0 mol kg⁻¹ NaOH at 298 K on ²⁹Si NMR spectra. In the **Si + Al** spectrum, for which aluminate is in large excess over solubility-limited silicate, only a single line (**2-4**) is seen at -75.0 ppm. This corresponds to the same 1:1 $[(HO)_3AlOSiO_2OH]^{3-}$ complex seen when $[Si] \gg [Al]$ ($\delta(Si^{29}) = -75.8^{28}$ or -76.2 at lower alkalinity⁴⁸). It may be inferred that, even with large excesses of aluminate, the

(48) Kinrade, S. D.; Swaddle, T. W. *Inorg. Chem.* **1989**, *28*, 1952.

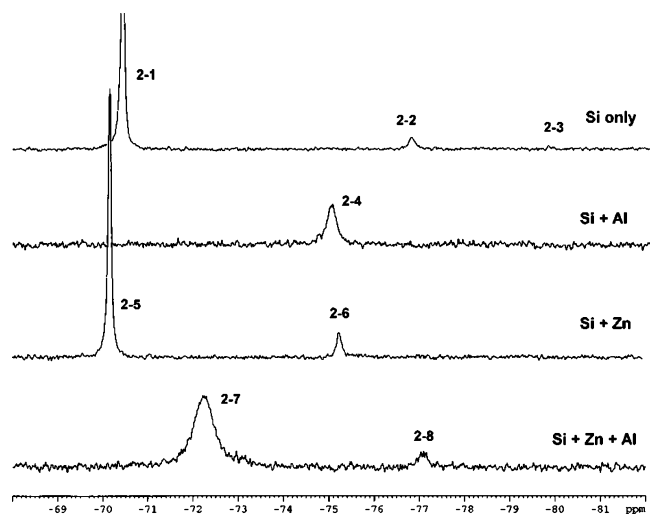


Figure 2. ^{29}Si NMR spectra showing the effect of zincate and aluminate on silicate ions in aqueous NaOH (15.0 mol kg^{-1} , 20% D_2O) at 298 K. Total concentrations (mol kg^{-1}): **Si only** spectrum, $[\text{Si}] = 1.09$; **Si + Al** spectrum, $[\text{Si}] = 0.065$, $[\text{Al}] = 1.61$; **Si + Zn** spectrum, $[\text{Si}] = 0.89$, $[\text{Zn}] = 0.89$; **Si + Zn + Al** spectrum, $[\text{Si}] = 0.59$, $[\text{Zn}] = 0.61$, $[\text{Al}] = 0.58$. Artificial line broadening = 1 Hz. Probe background has been subtracted. Vertical scales are arbitrary (not the same for all spectra). Peaks 2-1, 2-2, 2-3, 2-5, and 2-6 correspond to peaks 1-1, 1-2, 1-3, 1-7, and 1-8 in Figure 1.

complexation of aqueous silicate by aluminate does not proceed beyond 1:1, even though several aqueous aluminosilicate species with more Si atoms than Al atoms are known^{28,48} (cf. Loewenstein's rule⁴⁹). Line 2-4 is somewhat broadened (width 12.8 Hz) relative to 2-1 because of rapid chemical exchange with Al; the rates of such processes in aluminosilicates, although they are $\sim 10^4$ -fold faster than silicate–silicate exchange, are in the slow-exchange regime at 273 K when Si is in large excess over Al (i.e., when only a small fraction of the Si is present as relatively labile aluminosilicates),²⁸ but here it is Al that is in large excess.

The **Si + Zn** spectrum in Figure 2 shows two features, 2-5 and 2-6, attributable to $[(\text{HO})_3\text{ZnOSiO}_2\text{OH}]^{4-}$ and $[(\text{HO})_3\text{ZnO}(\text{SiO}_2)\text{O}(\text{SiO}_2)\text{OH}]^{6-}$, respectively. Spectrum **Si + Zn** is comparable to the case **Zn/Si = 0.98** in Figure 1, except for the higher alkalinity (with Na^+ instead of K^+) and temperature, which may explain the slightly more positive $\delta(^{29}\text{Si})$ values throughout Figure 2 as well as the absence of a feature analogous to peak 1-9.

Given that the ^{27}Al data imply that aluminate and zincate do not interact significantly with each other, the relative affinities of Si for Al and Zn were investigated by ^{29}Si spectroscopy by allowing Al and Zn to compete for a limited supply of silicate. When roughly equimolar amounts ($\sim 0.6 \text{ mol kg}^{-1}$) of Si, Zn, and Al are present together in 15 mol kg^{-1} NaOH (spectrum **Si + Zn + Al** in Figure 2), no new peaks emerge, but peaks derived from 2-5 and 2-6 move some 2.0 ppm to more negative $\delta(^{29}\text{Si})$ (peaks 2-7 and 2-8, respectively) and become substantially broadened, implying moderately rapid chemical exchange. That the broadness of 2-7 and 2-8 is the result of chemical exchange kinetics is shown by their temperature dependences (Figure

S3 in the Supporting Information); thus, for peak 2-7 at 280, 298, and 315 K, the respective line widths are 43, 31, and 13 Hz, with a negligible change in $\delta(^{29}\text{Si})$ (-72.2 ppm), as expected for resonances coalesced by chemical exchange.

Two possible interpretations of peak 2-7 are (i) that a new species, $[(\text{HO})_3\text{ZnO}(\text{SiO}_2)\text{OAl}(\text{OH})_3]^{5-}$, is formed and undergoes rapid chemical exchange with surplus $\text{Zn}(\text{OH})_4^{2-}$ and $\text{Al}(\text{OH})_4^-$ or (ii) that $\text{Zn}(\text{OH})_4^{2-}$ and $\text{Al}(\text{OH})_4^-$ compete roughly equally for the monomeric silicate, forming $[(\text{HO})_3\text{ZnOSiO}_2\text{OH}]^{4-}$ and $[(\text{HO})_3\text{AlOSiO}_2\text{OH}]^{3-}$ which give a broad coalesced ^{29}Si peak because of the chemical exchange involving these two species. The first alternative is less plausible. The experimental and theoretical data of Table 1, together with previous measurements,^{28,48} show that the conversion of a $\equiv\text{Si}-\text{O}-\text{H}$ function to $\equiv\text{Si}-\text{O}-\text{Al}(\text{OH})_3^-$ results in an average down frequency shift in $\delta(^{29}\text{Si})$ of about 4 ppm, in which case the ^{29}Si peak of the putative $[(\text{HO})_3\text{ZnO}(\text{SiO}_2)\text{OAl}(\text{OH})_3]^{5-}$ (species **M**, Table 1) would be expected to occur between -75 and -76 ppm on the basis of the observed $\delta(^{29}\text{Si})$ for species **J** (1-12). Furthermore, it was noted above that the maximum number of zincate or aluminate units that can separately complex monomeric silicate is evidently 1, and it is therefore unlikely that a zincate *and* an aluminate unit could together form a stable complex with a monomeric silicate center.

The second alternative would require the coalesced ^{29}Si resonance (frequency ν_{ZnAl}) of the $[(\text{HO})_3\text{ZnOSiO}_2\text{OH}]^{4-}$ and $[(\text{HO})_3\text{AlOSiO}_2\text{OH}]^{3-}$ ions to fall between the $\delta(^{29}\text{Si})$ values of these two ions in absence of each other (frequencies ν_{Zn} and ν_{Al}), dividing the frequency difference $\Delta\nu$ ($= \nu_{\text{Zn}} + \nu_{\text{Al}}$) in proportion to the mole fractions f_{Zn} and f_{Al} (where $f_{\text{Zn}} + f_{\text{Al}} = 1$) of these two ions in the solution

$$\nu_{\text{ZnAl}} = f_{\text{Zn}}\Delta\nu + \nu_{\text{Al}} \quad (3)$$

Figure 3, which shows the ^{29}Si NMR spectra of solutions with essentially constant stoichiometric $[\text{Si}]_{\text{total}}$ ($0.57 \pm 0.02 \text{ mol kg}^{-1}$) and excess $\{[\text{Al}] + [\text{Zn}]\}_{\text{total}}$ ($1.15 \pm 0.03 \text{ mol kg}^{-1}$) with variable $[\text{Zn}]/[\text{Al}]$ ratios at 298 K, demonstrates that this is at least qualitatively correct. The measured ^{29}Si NMR frequencies, ν_{ZnAl} , of peaks 3-1, 3-3, 3-5, and 3-7, together with ν_{Zn} and ν_{Al} , can therefore be inserted into eq 3 to calculate the true mole fractions, $f_{\text{Zn}}^{\text{NMR}}$ and $f_{\text{Al}}^{\text{NMR}}$, of $[(\text{HO})_3\text{ZnOSiO}_2\text{OH}]^{4-}$ and $[(\text{HO})_3\text{AlOSiO}_2\text{OH}]^{3-}$ because there is no NMR evidence of any unreacted silicate. Figure 4 shows that $f_{\text{Al}}^{\text{NMR}}$ is proportional to the stoichiometric f_{Al} but with a coefficient of 0.83, which implies that aluminate is somewhat less successful than zincate in competing for the limited supply of silicate under these conditions. Peaks 3-2, 3-4, 3-6, and 3-8, which comprise about 9.5% of the total Si, may be taken to represent the competition of zincate and aluminate for the silicate dimer and show the same qualitative trend, but quantitative analysis is not possible in absence of experimental data for the putative partner $[(\text{HO})_3\text{AlO}(\text{SiO}_2)\text{OSiO}_2\text{OH}]^{5-}$.

Detailed quantitative analysis of the phenomena shown in Figure 3 is not warranted, in particular because the limiting aluminosilicate spectrum had to be taken with a much lower

(49) Loewenstein, W. *Am. Mineral.* **1954**, *39*, 92.

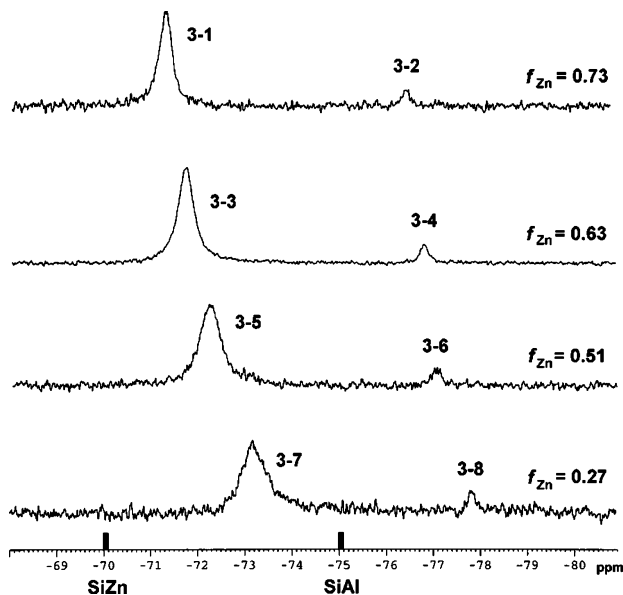


Figure 3. ^{29}Si NMR spectra of solutions of $\sim 0.57 \text{ mol kg}^{-1}$ silicate in 15.3 mol kg^{-1} NaOH containing total $\{\text{Zn} + \text{Al}\}$ concentrations of 1.15 mol kg^{-1} with varying stoichiometric mole fractions, f_{Zn} , of Zn, at 298 K. The ^{29}Si resonance frequencies of separate $[(\text{HO})_3\text{ZnOSiO}_2\text{OH}]^{4-}$ and $[(\text{HO})_3\text{AlOSiO}_2\text{OH}]^{3-}$ species are marked as SiZn and SiAl, respectively.

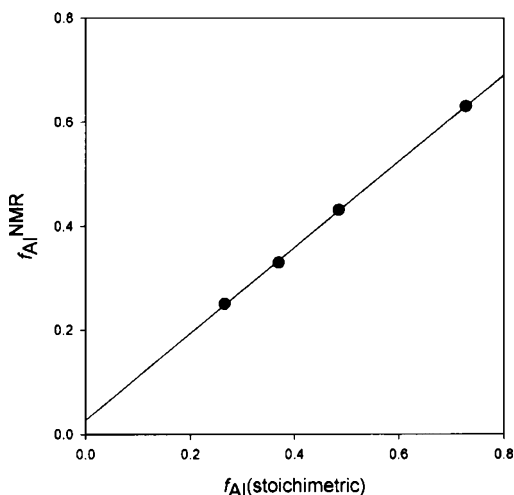


Figure 4. Relation of the mole fraction, $f_{\text{Al}}^{\text{NMR}}$, of $[(\text{HO})_3\text{AlOSiO}_2\text{OH}]^{3-}$ relative to $\{[(\text{HO})_3\text{ZnOSiO}_2\text{OH}]^{4-} + [(\text{HO})_3\text{AlOSiO}_2\text{OH}]^{3-}\}$, as determined by ^{29}Si NMR, to the stoichiometric mole fraction of total Al to total (Zn + Al). Slope = 0.83.

stoichiometric [Si] ($0.066 \text{ mol kg}^{-1}$) than the others because of solubility limitations and also showed substantial temperature-dependent line broadening (line widths 40.4, 12.8, and 5.7 Hz at 280, 298, and 315 K, respectively) indicative of some moderately rapid chemical exchange process involving aluminosilicate and excess aluminate. Furthermore, it is not clear how bound zincate and aluminate are distributed between complexes of the monomeric and dimeric silicate or what effects the excesses of unbound aluminate and zincate might have on ^{29}Si exchange. Nevertheless, a rough measure of the rate constant k for ^{29}Si exchange between $[(\text{HO})_3\text{ZnOSiO}_2\text{OH}]^{4-}$ and $[(\text{HO})_3\text{AlOSiO}_2\text{OH}]^{3-}$ (line widths in isolation W_{Zn} and W_{Al} , respectively) can be obtained from the line widths W_{AlZn} of peaks 3-1, 3-3, 3-5, and 3-7 if it is

assumed that the exchange rate is in the extreme line-narrowing region, for which eq 4 applies.

$$k = 4\pi f_{\text{Zn}} f_{\text{Al}} (\Delta\nu)^2 / (W_{\text{AlZn}} - f_{\text{Al}} W_{\text{Al}} - f_{\text{Zn}} W_{\text{Zn}}) C_{\text{Si}} \quad (4)$$

Here, C_{Si} is the sum of the Si in reactants $[(\text{HO})_3\text{ZnOSiO}_2\text{OH}]^{4-}$ and $[(\text{HO})_3\text{AlOSiO}_2\text{OH}]^{3-}$ (about 91% of $[\text{Si}]_{\text{total}}$). Data relevant to the estimation of k are given in Tables S1 and S2 (Supporting Information). The calculation is rather sensitive to W_{Al} if this is large, so that the data for 280 K in Table S1 should be disregarded. Moreover, the data of Table S2 suggest some dependence of the calculated k on residual Al and Zn. With these caveats, k can be estimated to be on the order of $3 \times 10^4 \text{ kg mol}^{-1} \text{ s}^{-1}$ at 298 K and $7 \times 10^4 \text{ kg mol}^{-1} \text{ s}^{-1}$ at 315 K.

Conclusions

Aqueous solutions containing sufficiently high Si, Al, and Zn concentrations for NMR spectroscopy can be prepared by resort to NaOH or KOH concentrations of 10–15 mol kg^{-1} , which also have the effect of limiting the number of small silicate species present to a tractable few (monomer, dimer, and cyclic trimer). In these media, complementary ^{29}Si and ^{67}Zn NMR spectra have provided evidence for the existence of several zincate–silicate complexes, notably $[(\text{HO})_3\text{ZnOSiO}_2\text{OH}]^{4-}$ and $[(\text{HO})_3\text{ZnO}(\text{SiO}_2)\text{O}(\text{SiO}_2)\text{OH}]^{6-}$, which undergo Si-site exchange that is rapid on the ^{29}Si NMR time scale because of the lability of the Zn^{II} centers. Zincate reacts incompletely and only slowly (on the ^{29}Si NMR time scale) with the cyclic trimer silicate because of the lack of $\equiv\text{Si}-\text{OH}$ groups for condensation on the latter at high pH. A maximum of one Zn^{II} can become attached to any silicate anion. ^{29}Si together with ^{27}Al NMR spectra show that zincate competes about equally (actually, a little more successfully) with aluminate for a deficiency of monomeric silicate to form coexisting $[(\text{HO})_3\text{ZnOSiO}_2\text{OH}]^{4-}$ and $[(\text{HO})_3\text{AlOSiO}_2\text{OH}]^{3-}$ which exchange Si with a rate constant on the order of $3 \times 10^4 \text{ kg mol}^{-1} \text{ s}^{-1}$ at 298 K.

The ability of aqueous silicate to scavenge Zn^{II} is therefore comparable to, or possibly a little better than, its well-established¹⁴ propensity for scavenging Al^{III} , at least in highly alkaline media. It is therefore likely that silicate anions released from psW and other bioactive ceramic implants at local pH 10.5 or less will also interact strongly with Zn^{II} as well as Al^{III} under physiological conditions, albeit with greater degrees of protonation of the $-\text{SiO}_x^{x-}$ groups than in our experiments.

Acknowledgment. T.W.S. and J.P.L. thank Qiao Wu for assistance with the NMR spectra and NSERC Canada for financial support. N.S. acknowledges the support of NSF through Grants EAR 0346689 and EAR 0208036. M.R.A. thanks Prof. R. Muller, Dr. S. Laurent, and Prof. A. Belayev for their support and helpful discussions. We thank the anonymous reviewers for helpful comments.

Supporting Information Available: ^{27}Al and ^{29}Si NMR spectra and tables of ^{29}Si chemical shifts and line widths. This material is available free of charge via the Internet at <http://pubs.acs.org>.

IC050594C